

# Crystal Structure of the Cytoplasmic Domain of the Type I TGF $\beta$ Receptor in Complex with FKBP12

Morgan Huse,\* Ye-Guang Chen,<sup>†§</sup>  
Joan Massagué,<sup>‡§</sup> and John Kuriyan\*<sup>†||</sup>

\*Laboratories of Molecular Biophysics

<sup>†</sup>Howard Hughes Medical Institute

Rockefeller University

New York, New York 10021

<sup>‡</sup>Cell Biology Program

<sup>§</sup>Howard Hughes Medical Institute

Memorial Sloan Kettering Cancer Center

New York, New York 10021

## Summary

Activation of the type I TGF $\beta$  receptor (T $\beta$ R-I) requires phosphorylation of a regulatory segment known as the GS region, located upstream of the serine/threonine kinase domain in the cytoplasmic portion of the receptor. The crystal structure of a fragment of unphosphorylated T $\beta$ R-I, containing both the GS region and the catalytic domain, has been determined in complex with the FK506-binding protein FKBP12. T $\beta$ R-I adopts an inactive conformation that is maintained by the unphosphorylated GS region. FKBP12 binds to the GS region of the receptor, capping the T $\beta$ R-II phosphorylation sites and further stabilizing the inactive conformation of T $\beta$ R-I. Certain structural features at the catalytic center of T $\beta$ R-I are characteristic of tyrosine kinases rather than Ser/Thr kinases.

## Introduction

Transforming growth factor  $\beta$  (TGF $\beta$ ) is the founding member of a set of secreted, dimeric, peptide growth factors that includes the TGF $\beta$ s, activins, inhibins, bone morphogenic proteins (BMPs), and others (Massagué, 1990; Roberts and Sporn, 1990). Once secreted and activated, TGF $\beta$  signals by engaging a specific cell surface receptor composed of two related transmembrane serine/threonine kinases, called the type I and type II TGF $\beta$  receptors (T $\beta$ R-I and T $\beta$ R-II), respectively (Heldin et al., 1997; Massagué, 1998). T $\beta$ R-I and T $\beta$ R-II have the same basic structural elements: a cysteine-rich N-terminal extracellular domain, which is involved in ligand binding; a single transmembrane helix; and a C-terminal cytoplasmic kinase domain. In addition, T $\beta$ R-I, but not T $\beta$ R-II, contains a regulatory segment in its cytoplasmic juxtamembrane region called the GS region or domain (named for the conserved <sup>185</sup>TTSGSGSGLP<sup>194</sup> sequence at its center). The basic mechanism of TGF $\beta$  receptor activation has been established (Wrana et al., 1994; Chen and Weinberg, 1995). The type II receptor binds ligand first and then recruits the type I receptor. Next, T $\beta$ R-II phosphorylates serine and threonine residues in the GS region of T $\beta$ R-I (Wrana et al., 1994).

These multiple phosphorylation events activate the type I receptor kinase, which transduces the signal by phosphorylating and activating members of the Smad family of transcription factors (Massagué, 1998).

Transmembrane receptors for polypeptide ligands typically signal by the activation of associated tyrosine kinase domains. In contrast, the TGF $\beta$  family of receptors phosphorylates serine and threonine residues. Sequence comparisons have shown that while the catalytic domains of TGF $\beta$  receptor kinases contain sequence motifs that are characteristic of Ser/Thr kinases, this family clusters close to the tyrosine kinases in terms of overall sequence similarity (Hanks and Hunter, 1995). This raises the possibility that the TGF $\beta$  receptor family represents a link in the evolution of tyrosine kinases.

Many receptor tyrosine kinases are activated by phosphorylation of the activation loop or segment, a central structural element within the kinase domain (Johnson et al., 1996). This is not the case for T $\beta$ R-I. Instead, kinase activation is achieved by multiple phosphorylations in the GS region, upstream of the catalytic domain (Wrana et al., 1994). This mechanism of activation is unique to the TGF $\beta$  receptor family, and there is consequently no structural precedent for understanding the molecular basis for the control of T $\beta$ R-I kinase activity.

Several different type I receptors have been shown to interact strongly with the immunophilin FKBP12 (Wang et al., 1994; Okadome et al., 1996). FKBP12 plays a crucial role in mediating the effects of the immunosuppressant drugs FK506 and rapamycin (Schreiber, 1991). Its normal biological function is not completely established, and the physiological relevance of the binding of T $\beta$ R-I by FKBP12 remains controversial (Charng et al., 1996; Shou et al., 1998). FKBP12 binding has been shown to inhibit TGF $\beta$  receptor-mediated signaling (Wang et al., 1996; Chen et al., 1997; Stockwell and Schreiber, 1998b), and it has been proposed that FKBP12 serves to eliminate spurious signaling caused by receptor oligomerization in the absence of ligand (Chen et al., 1997).

A detailed mechanistic understanding of the regulation of the TGF $\beta$  family receptors has been hindered by the lack of three-dimensional structural information on this class of protein kinases. We now present the crystal structure of the unphosphorylated cytoplasmic domain of the type I TGF $\beta$  receptor (T $\beta$ R-I) in complex with FKBP12. The T $\beta$ R-I kinase adopts an inactive conformation, which is maintained by interactions between the GS region, the activation segment, and the N-terminal lobe of the kinase. The structure shows that phosphorylation of the GS region would disrupt its conformation, thereby relieving the inhibitory interactions. FKBP12 binds to the GS region, protecting the T $\beta$ R-II phosphorylation sites and stabilizing the inhibited conformation of the kinase. Finally, an intriguing structural connection is established between the catalytic center of T $\beta$ R-I and those of tyrosine kinases.

<sup>||</sup> To whom correspondence should be addressed (e-mail: [kuriyan@rocky2.rockefeller.edu](mailto:kuriyan@rocky2.rockefeller.edu)).

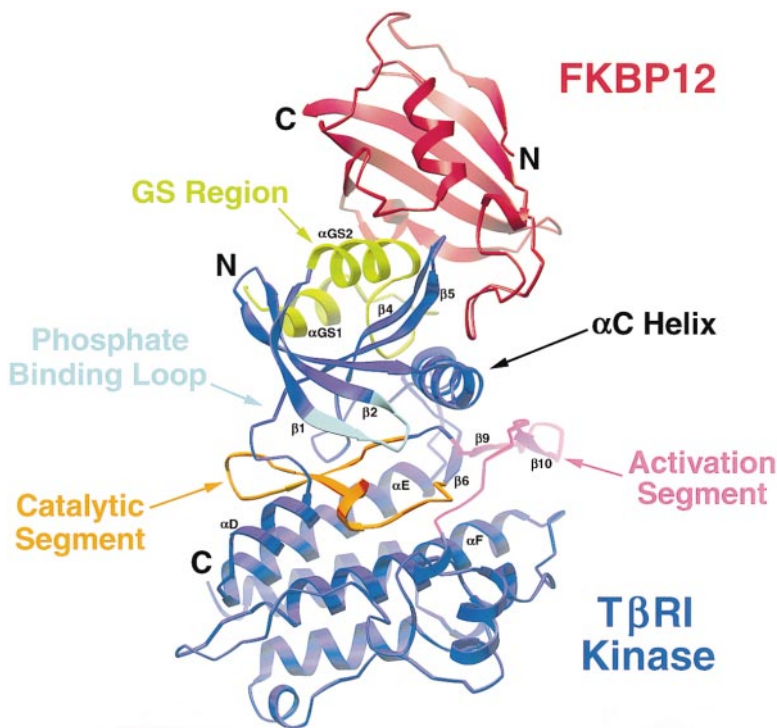


Figure 1. The Structure of T $\beta$ R-I in Complex with FKBP12

All elements of secondary structure discussed in the text are labeled. This figure and all subsequent RIBBONS diagrams were generated using RIBBONS (Carson, 1991).

## Results and Discussion

### Structure Determination and Basic Architecture of the T $\beta$ R-I Kinase

A fragment comprising residues 162–503 of human T $\beta$ R-I (hereafter referred to as T $\beta$ R-I) was expressed and purified from insect cells. The T $\beta$ R-I protein forms a stable complex (1:1) with human FKBP12. Crystals of the complex are triclinic, with four complexes in the asymmetric unit. The structure of the complex (Figure 1) was solved by multiple isomorphous replacement (MIR, see Experimental Procedures). The current model has been refined to an R value of 24.9% and a free R value (Brünger, 1992) of 26.9%, using data to a resolution of 2.6 Å.

The core region of the T $\beta$ R-I catalytic domain (residues 205–500) adopts a canonical protein kinase fold, similar to that first seen in the structure of the cAMP-dependent protein kinase PKA (Knighton et al., 1991). A smaller N lobe is involved in ATP binding, and a larger C lobe is required for substrate recognition. The N lobe is dominated by a twisted, five-stranded  $\beta$  sheet, while the C lobe is largely helical (Figure 1). The N-terminal GS region forms a helix-loop-helix segment that is packed tightly onto the outer surface of the  $\beta$  sheet of the N lobe. FKBP12 is bound to the GS region. In the N lobe, type I receptors contain an insertion between strands  $\beta$ 4 and  $\beta$ 5 (the L45 loop) that determines Smad substrate specificity (Feng and Derynck, 1997; Chen et al., 1998). The L45 loop extends out into solution, where it is well positioned to interact with other proteins (Figure 4B). Close sequence similarity between various type I receptors (the T $\beta$ R-I catalytic domain shares 90% identity with activin receptor-IB, 68% with BMP receptor-IB) and between type I and type II receptor kinase domains

(41% identity with T $\beta$ R-II) allows the structure presented here to serve as a useful model for TGF $\beta$  receptors in general.

### The T $\beta$ R-I Kinase Domain Is in an Inactive Conformation

Comparison of the structure of the T $\beta$ R-I kinase domain with that of the active Ser/Thr kinase PKA reveals several features in the T $\beta$ R-I kinase that would impair its catalytic activity. The catalytic segment is a highly conserved and centrally located loop within the protein kinase domain that connects the E helix and the activation segment (Figures 1 and 2). If T $\beta$ R-I and PKA are aligned using only their catalytic segments (residues 331–351 in T $\beta$ R-I, 164–184 in PKA), it becomes apparent that the N lobe of T $\beta$ R-I is shifted away from the active configuration seen in PKA (Figure 3A). The bulk of this movement consists of a 7° rigid body rotation about an axis roughly perpendicular to the N-terminal  $\beta$  sheet of the kinase domain. This rotation results in a shearing of the active site (Figure 3B). Lys-232 and Glu-245, two catalytic groups contributed by the N lobe, are moved by  $\sim$ 3 Å with respect to residues contributed by the catalytic segment, namely Asp-333, Asn-338, and Asp-351.

Protein kinases engage ATP in a deep groove between their N and C lobes. In T $\beta$ R-I, the rotation and distortion of the N lobe damages the integrity of the ATP-binding site. In particular, the phosphate and magnesium recognition pocket is constricted. The nucleotide from the PKA structure can be docked into T $\beta$ R-I based on the alignment of catalytic segments. When this is done, it becomes apparent that the space occupied by the phosphate groups in the nucleotide-binding site of PKA is occluded in T $\beta$ R-I by elements of the N lobe  $\beta$  sheet

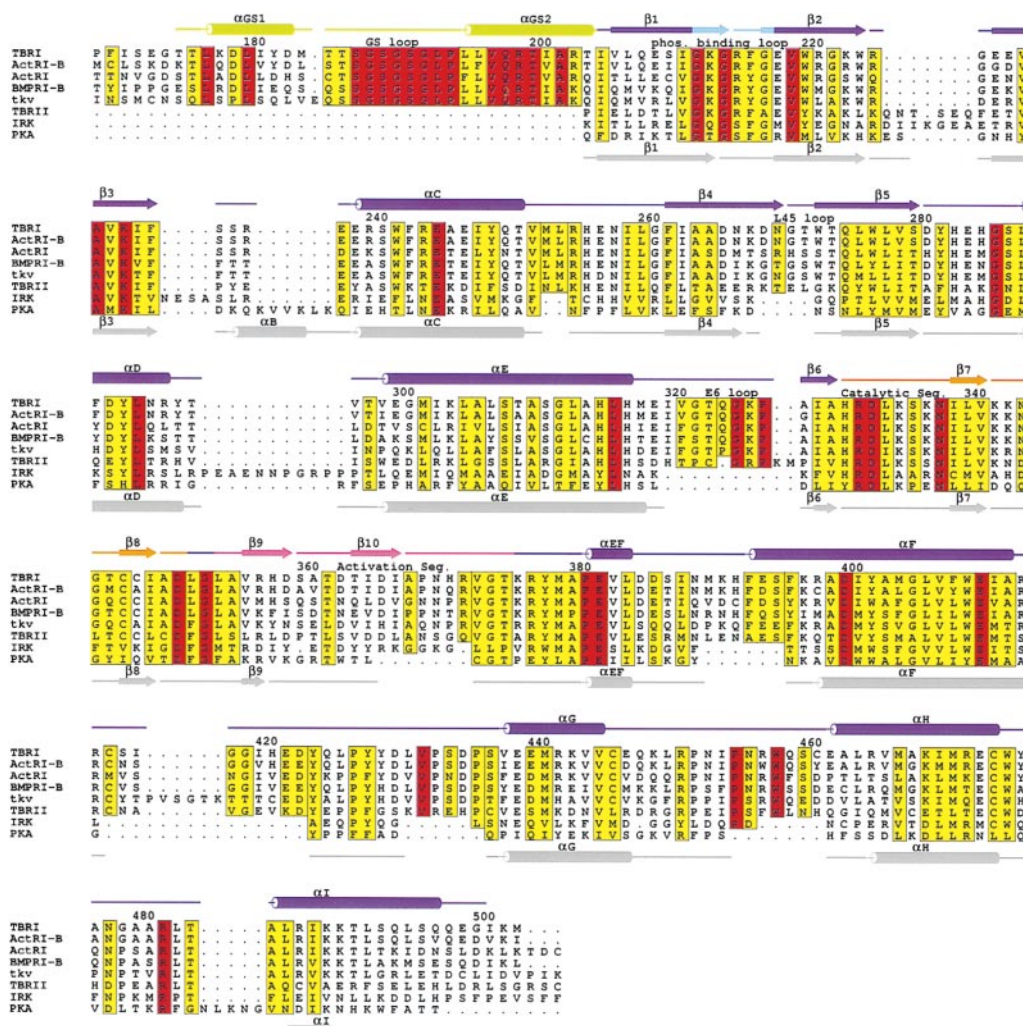


Figure 2. An Alignment of T $\beta$ R-I with Other Protein Kinases

The sequence of the T $\beta$ R-I cytoplasmic domain is aligned with that of other type I receptors and with T $\beta$ R-II. Structure-based alignments against PKA and IRK are also shown. Secondary structural elements of T $\beta$ R-I, colored as in Figure 1, are shown directly above the alignment, with cylinders indicating helices and arrows indicating  $\beta$  strands. The secondary structure of PKA is shown below the alignment. Structural elements are named as in PKA (Knighton et al., 1991). In the alignment, red represents absolute sequence identity over all sequences present in that part of the alignment, while yellow represents a similarity score of 5 using the method of Livingston and Barton (1996). Alignment generated using Alscript (Livingston and Barton, 1996).

(Figure 3C). Lys-232 blocks the binding of the  $\alpha$ -phosphate, Phe-216 blocks the  $\beta$ -phosphate, and Phe-216 together with Arg-372 block the  $\gamma$ -phosphate.

The role of Arg-372 in disrupting the active site is particularly interesting. Arg-372 is a residue in the activation segment that extends its side chain into the catalytic center to form an ion pair with Asp-351 (Figure 3B), a ligand for a crucial magnesium ion (Armstrong et al., 1979; Zheng et al., 1993). The Arg-372–Asp-351 interaction effectively disrupts magnesium binding. The T $\beta$ R-I–FKBP12 crystals used in this study were grown in the presence of AMP–PNP and magnesium. Convincing density for the nucleotide and Mg<sup>2+</sup> ions has not been obtained, which is consistent with the partial blockage of the ATP-binding site observed in this structure.

The observed misorientation of the active site and ATP-binding groove in T $\beta$ R-I appears to be a fairly gentle

form of autoinhibition when compared with the larger distortions seen in certain other inhibited kinases (Hu et al., 1994; Goldberg et al., 1996; Russo et al., 1996). Consistent with this, unphosphorylated T $\beta$ R-I displays very low but detectable activity in kinase assays (data not shown). This small amount of activity, while insignificant in any catalytic sense, has been sufficient in previous studies to map phosphorylation sites on downstream Smad proteins (Kretzschmar et al., 1997).

#### Structural Stabilization of the Inactive Conformation

In T $\beta$ R-I, the catalytically inactive conformation appears to be maintained by interactions between the N lobe of the kinase, the GS region, and the activation segment. In particular, the GS region and the activation segment act together to position and stabilize the  $\alpha$ C helix such that it tips into and pins back the  $\beta$  sheet of the N



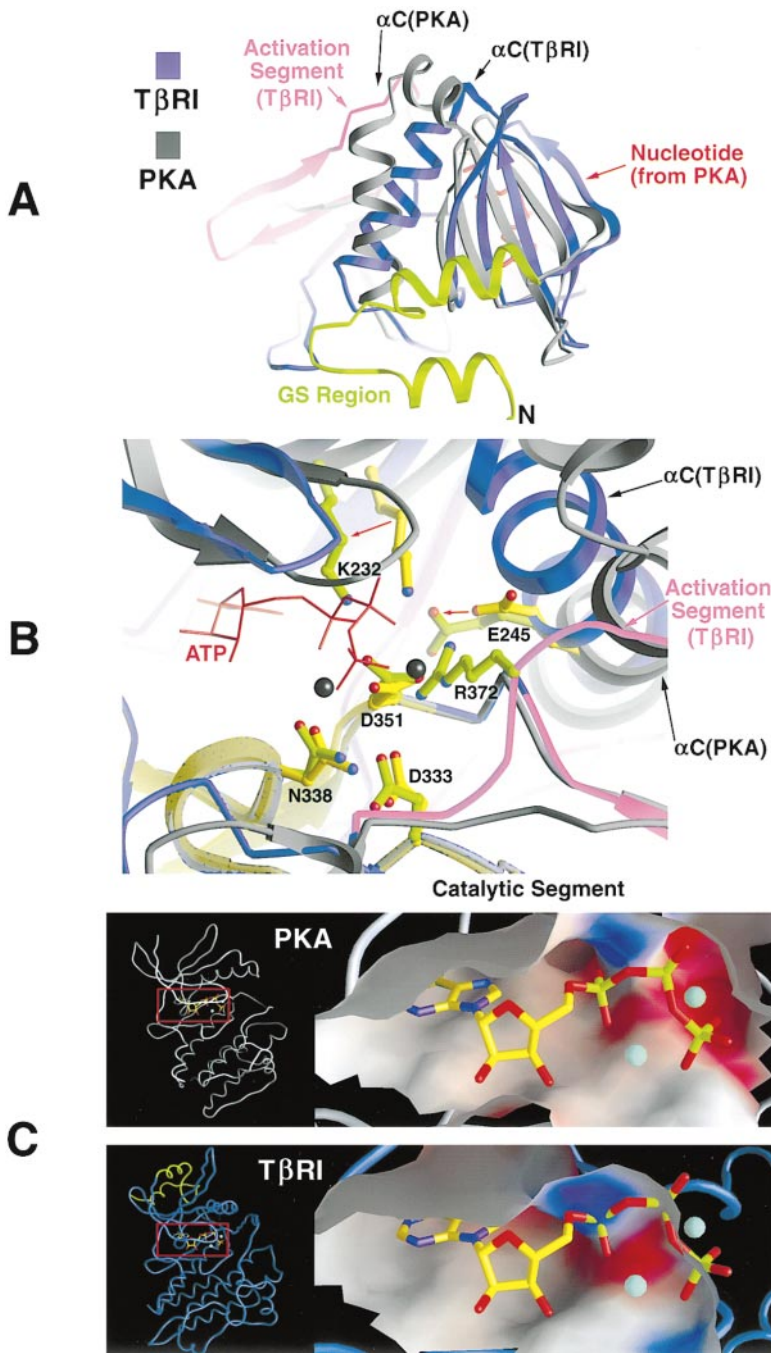


Figure 3. The TβR-I Kinase Adopts an Inactive Conformation

TβR-I and PKA (Zheng et al., 1993) were aligned for this figure using their kinase catalytic segments.

(A) The TβR-I-PKA alignment viewed from above the β sheet of the N lobe. The N lobe β sheet of TβR-I is rotated with respect to PKA. (B) A view of the TβR-I-PKA alignment showing the active site and several conserved catalytic residues. The proteins are colored as in (A), with ATP from the PKA structure represented in red sticks. The aligned catalytic segments have been highlighted. The two metal ions found in the PKA structure are shown as black balls. TβR-I residues are colored green, and PKA residues are colored yellow. Side chains are labeled using TβR-I numbering. The corresponding residues in PKA are K72, E91, D166, N171, and D184. The TβR-I active site is sheared relative to PKA, and red arrows indicate the resulting displacements of K232 and E245. In addition, the Arg-372-Asp-351 ion pair disrupts the innermost metal-binding site.

(C) A comparison of the PKA and TβR-I ATP-binding sites. PKA is shown above in complex with ATP and metal ions. TβR-I is shown below, with the nucleotide and metal ions from PKA docked into its active site based on the catalytic segment alignment. The regions boxed to the left have been magnified on the right. Electrostatic surface representations of the ATP-binding pockets have been included, with blue indicating positive potential and red indicating negative potential. The two metal ions are shown in cyan. The surface representations show that there is no room for the ATP phosphate groups or the innermost metal ion in the TβR-I nucleotide-binding pocket. These and other molecular surfaces were generated using GRASP (Nicholls et al., 1991).

lobe (Figure 3A). Relative to its configuration in active kinases, the C-terminal portion of αC lies further from the β sheet by 2–3 Å, while the N-terminal end is pressed closer to a similar extent.

We refer to the two helices in the GS region as αGS1 and αGS2. Helix αGS2 nestles in the groove created by the twisted β sheet of the N lobe and engages in an array of contacts with the top of the β sheet and the amphipathic αGS1 helix, forming a hydrophobic core (Figure 4A). FKBP12 binds directly to the GS2 helix and appears to further reinforce the conformation of the GS region. The network of hydrophobic interactions within the GS region suggests that its conformation is stable

in the absence of FKBP12 binding and is not induced by it. The loop connecting αGS1 and αGS2 (the GS loop) spans the conserved <sup>185</sup>TTS<sup>194</sup> sequence motif, which contains sites that are phosphorylated by the type II receptor. The GS loop forms a wedge that inserts into the space between the αC helix and the β4 strand of the N lobe, with the side chain of Ser-191 extending into the very base of the cavity (Figure 4B). There is a two-residue insertion in the kinase domain that is conserved among type I receptors, which maps to the C terminus of the TβR-I αC helix (Figure 2). This insertion allows the C helix to move away from strand β4, creating the space required for GS loop insertion.

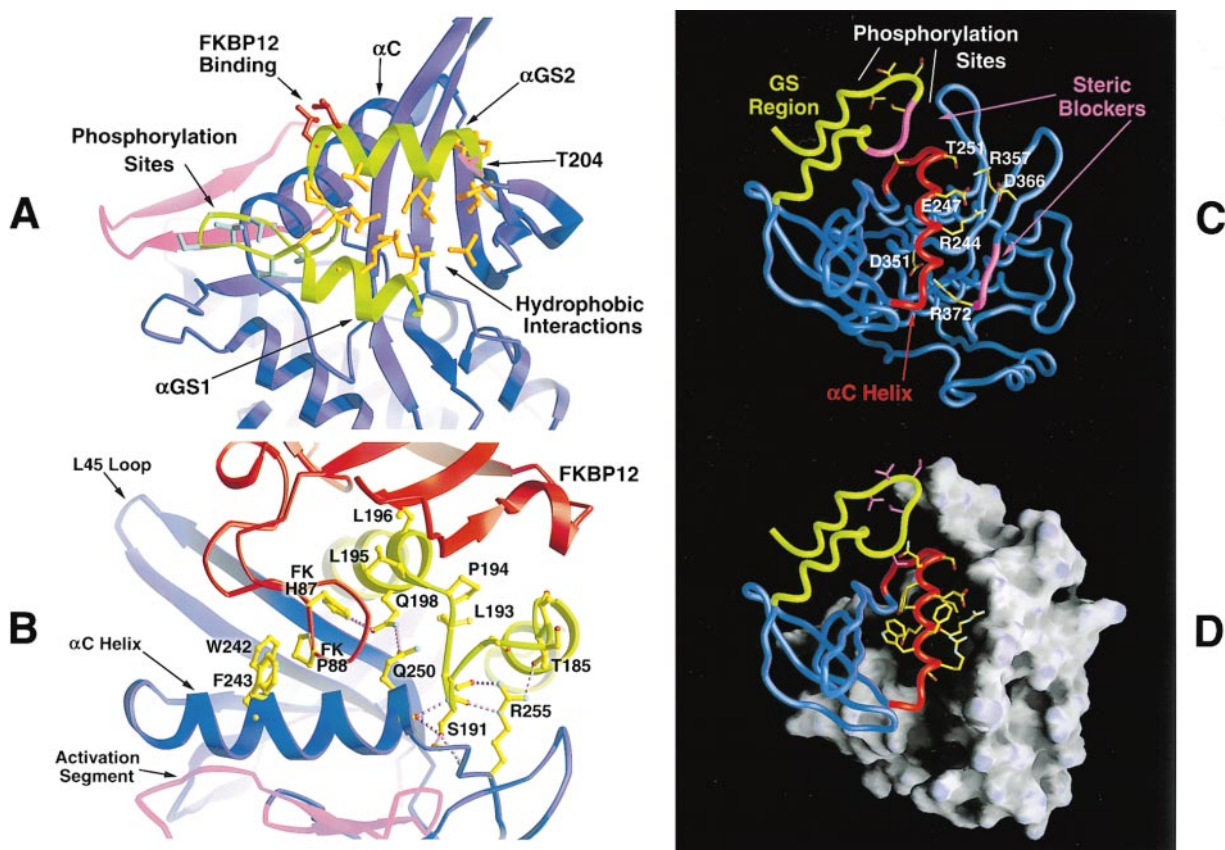


Figure 4. The Inhibited Conformation of T $\beta$ R-I Is Maintained by the GS Region and the Activation Segment

(A) A ribbon drawing showing the hydrophobic interactions made between the GS region helices and the top of the kinase  $\beta$  sheet. T $\beta$ R-I is viewed from above the kinase N lobe. Thr-204, the site of a constitutively activating T $\beta$ R-I mutation (Wieser et al., 1995), is indicated.

(B) A ribbon drawing of the complex showing interactions between the GS loop and the T $\beta$ R-I kinase, as well as contacts formed between FKBP12 and T $\beta$ R-I. Several interacting residues are shown, with hydrogen bonding indicated by dashed purple bonds. The L45 loop is indicated.

(C) T $\beta$ R-I viewed from an oblique angle above the kinase N lobe. The T $\beta$ R-II phosphorylation sites are indicated, as are several residues involved in ionic or polar interactions that stabilize the placement of the C helix. The movement of the C helix and the N lobe  $\beta$  sheet into an active conformation appears to be blocked by the GS loop and a short stretch within the activation segment. These two steric blockers have been colored magenta.

(D) The same view as in (C), with a molecular surface representation of the kinase C lobe. The  $\alpha$ C side chains have been included to indicate the space occupied by the helix. The outward rotation of the C helix and the N lobe  $\beta$  sheet is blocked by the barrier created by the activation segment.

The T $\beta$ R-I activation segment forms a  $\beta$  hairpin (consisting of strands  $\beta$ 9 and  $\beta$ 10) that is supported by a one and a half turn extension of the  $\alpha$ F helix (Figures 1 and 2).  $\beta$ 9 and  $\beta$ 10, together with strand  $\beta$ 6, form a three-stranded sheet that cradles the C helix and appears to stabilize its rotated conformation (Figures 1, 4C, and 4D). Residues from this  $\beta$  sheet interact with  $\alpha$ C over much of its length. The side chains of Ile-248 and Val-252 from  $\alpha$ C make van der Waals contacts with Ile-329 and Pro-327 from strand  $\beta$ 6. Glu-247 positions Arg-244 to interact with Asp-366 in strand  $\beta$ 10. Asp-366, in turn, fixes Arg-357 from  $\beta$ 9 to properly hydrogen bond with Thr-251.

The interactions between the  $\alpha$ C helix, the GS region, and the activation segment restrict the motion of the helix (Figure 4C and 4D). Two elements (residues 368–372 in the activation segment and residues 189–192 in the GS loop) act as steric blockers that cage the  $\alpha$ C

helix. The activation segment also contacts the N lobe  $\beta$  sheet directly. The side chain of Phe-216, a residue in the loop connecting strands  $\beta$ 1 and  $\beta$ 2, is in van der Waals contact with the aliphatic portion of Arg-372. Any activating rotation of the kinase N lobe would produce a steric clash between these residues.

#### Activation of T $\beta$ R-I

The unphosphorylated GS loop adopts an unusual conformation in which the protein chain undergoes two 180° turns in the space of seven residues (Figures 4A and 4B). It is unlikely that the GS loop will maintain this partially buried and tightly folded conformation upon the addition of bulky and negatively charged phosphate groups. Release of the GS region from this internally bound configuration will presumably relieve the inhibitory effects of the GS loop on the C helix and N-terminal kinase  $\beta$  sheet.

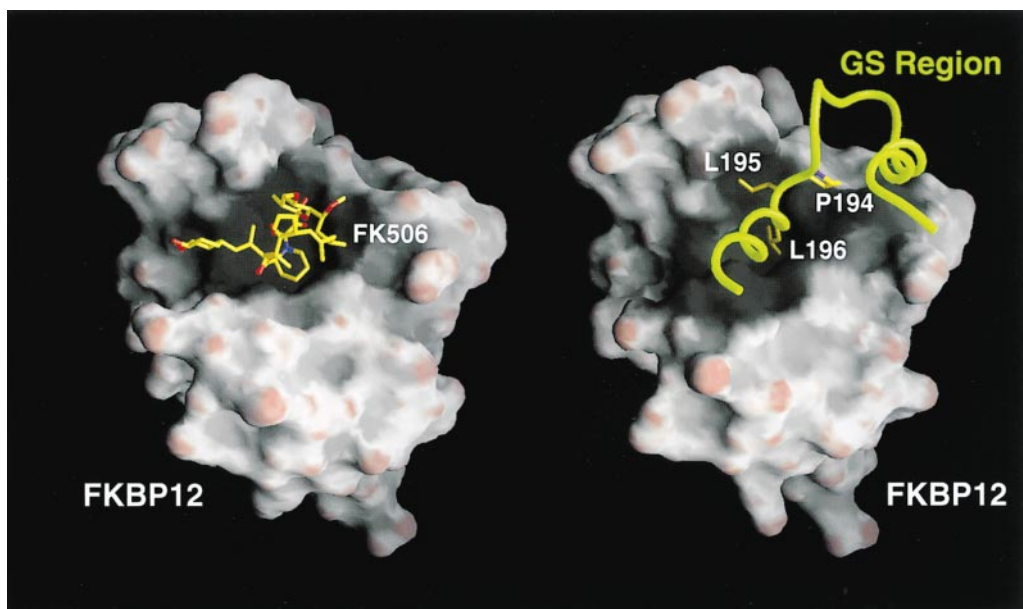


Figure 5. A Comparison of the FKBP12-FK506 and FKBP12-T $\beta$ R-I Complexes

A surface representation of FKBP12 bound to FK506 is shown to the left (Wilson et al., 1995). To the right is shown a surface representation of FKBP12 bound to the T $\beta$ R-I GS region. Leu-195 and Leu-196 are bound in the same hydrophobic pocket used to engage immunosuppressant.

A number of mutagenesis studies aimed at clarifying the role of the GS region in activation have been performed (Feng et al., 1995; Wieser et al., 1995; Willis et al., 1996). Some of these results suggest that the GS region, in addition to playing an inhibitory role when unphosphorylated, may also adopt a distinct activating conformation upon phosphorylation. For example, deletion of the entire juxtamembrane region of T $\beta$ R-I, including the GS region, results in an inactive receptor, implying that a phosphorylated GS loop may be required in the active state (Feng et al., 1995). Mutation of the serines and threonines in the GS loop to aspartate destroys signaling activity in T $\beta$ R-I (Wieser et al., 1995), suggesting that the activated GS loop conformation places particular structural requirements on these residues in addition to negative charge. Substitution of Thr-204 with aspartate or glutamate creates a type I receptor that is constitutively active and independent of the type II receptor (Wieser et al., 1995; Willis et al., 1996). Thr-204 lies at the C terminus of the GS2 helix, well away from the GS loop and the catalytic center, and its role in activation is not apparent from this structure (Figure 4A). The molecular basis for these observations may only become clear upon analyzing the conformation of the GS region in the active, oligomeric receptor complex.

The configuration of the activation segment will also have to change in order to relieve the steric blockage to N lobe rotation and to remove Arg-372 from the active site. Many kinases are activated by direct phosphorylation of the activation segment, which leads to a restructuring that enables kinase activity (Johnson et al., 1996). T $\beta$ R-I contains two threonine residues (362 and 364) that are potential sites for such phosphorylation. Phosphopeptide mapping of phosphorylated sites in activated receptor complexes has revealed no evidence

for phosphorylation in this region (Wrana et al., 1994; Souchelnytskyi et al., 1996). Furthermore, mutation of either Thr-362 or Thr-364 to alanine or aspartate, as well as mutation of both together, produces no significant change in TGF $\beta$ -induced signaling (data not shown), indicating that activation segment phosphorylation is not required for receptor activation. Possible mechanisms for modulating the conformation of the activation segment include interactions between the phosphorylated GS region and the activation segment, changes in the quaternary arrangement of protomers within the oligomeric receptor complex, or substrate binding.

#### The T $\beta$ R-I-FKBP12 Interaction

The T $\beta$ R-I-FKBP12 structure is the first that captures FKBP12 bound directly to a protein target. The conformation of FKBP12 in the T $\beta$ R-I-FKBP12 complex is essentially identical to that of FKBP12 seen in other structures (rmsd of 0.52 Å over C $\alpha$  positions relative to FKBP12 bound to FK506, 0.63 Å for FKBP12 bound to FK506 and calcineurin) (Van Duyne et al., 1991; Griffith et al., 1995; Wilson et al., 1995). Two conserved residues in the T $\beta$ R-I GS region, Leu-193 and Pro-194, are known to be required for FKBP12 binding (Chang et al., 1996; Chen et al., 1997). The presence of a crucial proline in the binding region is intriguing, since FKBP12 has proline rotamase activity (Harrison and Stein, 1990). However neither Leu-193 nor Pro-194 interacts directly with FKBP12 in the structure of the complex. Rather, these two residues appear to be important for stabilizing the interface.

FKBP12 binds directly to Leu-195 and Leu-196, two highly conserved residues situated at the N-terminal tip of the GS2 helix (Figure 2). It accommodates the two aliphatic side chains in the same hydrophobic binding



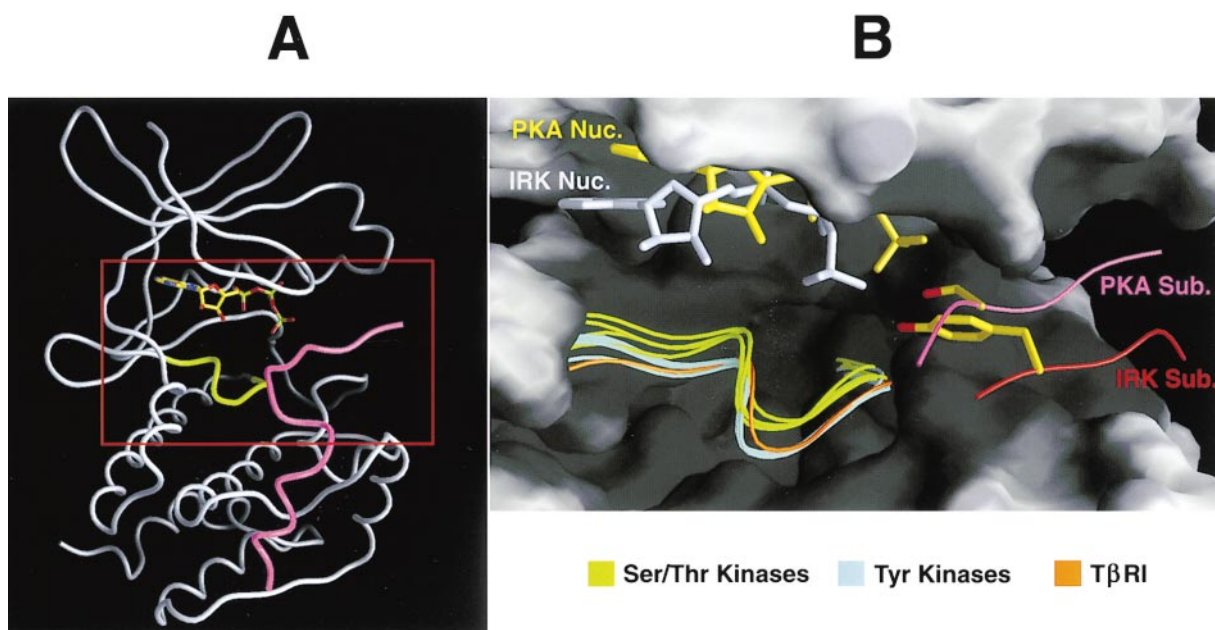


Figure 6. The T $\beta$ R-I C Lobe Has Tyrosine Kinase-like Features

(A) A ribbon representation of PKA (Zheng et al., 1993) showing bound ATP and PKI substrate analog. The portion of the catalytic segment (residues 164–172 in PKA) analyzed in (B) is colored green.

(B) The boxed region in (A) has been magnified to show the kinase active site. The N lobe and C lobe of PKA are shown in surface representation. The catalytic segments of four Ser/Thr kinases (PKA, phosphorylase kinase, the MAP kinase p38, and Cdk2) (Zheng et al., 1993; Jeffrey et al., 1995; Owen et al., 1995; Wang et al., 1997), four Tyr kinases (IRK, Hck, Src, and the FGF receptor) (Mohammadi et al., 1996; Hubbard, 1997; Sicheri et al., 1997; Xu et al., 1997), and T $\beta$ R-I are shown based on an alignment of their C lobe helices. PKI and the IRK substrate are shown as representative Ser/Thr and Tyr kinase substrates, respectively. A hypothetical serine has been modeled onto PKI using the position of Ala-21. Nucleotides from the active PKA and IRK structures are also included. The catalytic segments cluster into two groups, and T $\beta$ R-I clusters with the Tyr kinases.

pocket used to engage macrolide (Figure 5), which is consistent with the ability of both rapamycin and FK506 to relieve FKBP12-mediated inhibition of TGF $\beta$  signaling (Okadome et al., 1996; Wang et al., 1996; Chen et al., 1997; Stockwell and Schreiber, 1998b). Leu-195 occupies the same space as would the hemiketal ring of FK506, while Leu-196 substitutes for the pipercolinyl moiety. FKBP12 makes additional contacts with T $\beta$ R-I outside of the FK506-binding site (Figure 4B), and many of these interactions are likely to be conserved in other type I receptors.

It has been proposed that FKBP12 inhibits TGF $\beta$  signaling by occluding the type II receptor phosphorylation sites in the type I receptor GS region (Chen et al., 1997). While FKBP12 makes no direct contacts with residues in the GS loop, it is positioned close enough to impede the approach of a T $\beta$ R-II kinase domain. Given the close proximity of FKBP12 to the GS loop, it is also plausible that GS loop phosphorylation induces FKBP12 dissociation, as has been suggested (Wang et al., 1996; Chen et al., 1997).

A recent report has detailed the analysis of FKBP12-null mice (Shou et al., 1998). No apparent defect in TGF $\beta$  signaling was observed in fibroblasts taken from these mice, and the authors suggest that the T $\beta$ R-I-FKBP12 interaction has no physiological relevance. This conclusion may be too strong. Indeed, a number of studies have shown that FKBP12 dissociation, while not sufficient, is necessary for T $\beta$ R-I activation (Wang et al.,

1996; Chen et al., 1997; Stockwell and Schreiber, 1998b). FKBP12 appears to act as a buffer, rather than an outright antagonist, of the TGF $\beta$  system, stabilizing and prolonging the lifetime of downregulated T $\beta$ R-I. The T $\beta$ R-I-FKBP12 structure is consistent with this role. As has been suggested (Stockwell and Schreiber, 1998b), such a buffering function may only become important when receptor concentration is high enough to make ligand-independent activation a problem.

#### A Structural Link between T $\beta$ R-I and Tyrosine Kinases

Comparison of the structures of the active serine/threonine kinase PKA (Zheng et al., 1993) and the active tyrosine kinase insulin receptor kinase (IRK) (Hubbard, 1997) reveals that tyrosine kinases bind peptide substrate further down in their C lobe (Figure 6). This change allows tyrosine kinases to interpose the C-terminal end of their activation segment between the substrate and the active site, thereby holding the substrate further away and providing a molecular basis for tyrosine specificity (Hubbard et al., 1994; Hubbard, 1997). This lowering of substrate peptide is mirrored by a  $\sim 1$  Å drop in the catalytic segment of tyrosine kinases with respect to the rest of the C lobe, which brings the entire ATP-binding site and catalytic center down to the level of the substrate. The change in the placement of the catalytic segment relative to the C lobe results in a compensatory movement of the  $\alpha$ E helix, which bulges out at its N

terminus. These structural changes relative to Ser/Thr kinases are conserved in all Tyr kinases of known structure.

When the  $\alpha$  helices in the C lobe of T $\beta$ R-I are superimposed with those of other kinases, it becomes apparent that T $\beta$ R-I displays the same catalytic segment lowering and E helix bulge characteristic of tyrosine kinases (Figure 6). T $\beta$ R-I is able to phosphorylate serine and threonine because it lacks a conserved proline (Pro-1172 in IRK), which, in tyrosine kinases, kinks the activation segment such that substrate is held further from the active site. The tyrosine kinase-like disposition of the catalytic segment and the C lobe, however, may explain how the TGF $\beta$  type II receptor can function as a dual specificity kinase, at least under certain conditions in vitro (Lawler et al., 1997).

The protein kinase of known structure most closely related to T $\beta$ R-I in terms of overall sequence identity is the tyrosine kinase IRK, which shares 30% identity with T $\beta$ R-I over  $\sim$ 250 aligned residues (Figure 2). The sequence identity between T $\beta$ R-I and Ser/Thr kinases is lower (e.g.,  $\sim$ 22% versus PKA, ERK2, and Cdk2). The closer similarity between IRK and T $\beta$ R-I in terms of sequence is reflected in the three-dimensional structure. The  $\alpha$  helices in the C lobe of T $\beta$ R-I can be superimposed upon the corresponding helices in IRK (Hubbard, 1997) with a root-mean-square deviation of 1.3 Å for 102 C $\alpha$  atoms. The deviation for a similar alignment with PKA (Zheng et al., 1993) is 1.8 Å.

The similarity between TGF $\beta$  family receptors and tyrosine kinases suggests that an ancestor of the former may represent a branch point in the evolution of tyrosine kinases from cytoplasmic serine/threonine kinases. Interestingly, a transmembrane serine/threonine kinase has been discovered in yeast. This protein, called Ire1p, is involved in the unfolded protein response (Shamu and Walter, 1996). However, the sequence of its kinase domain does not obviously place it in the TGF $\beta$  receptor superfamily (Hanks and Hunter, 1995).

#### A Noncrystallographic T $\beta$ R-I Dimer

The active TGF $\beta$  receptor complex contains homodimers (or higher oligomers) of T $\beta$ R-I in addition to homooligomers of T $\beta$ R-II (Chen and Derynck, 1994; Henis et al., 1994; Yamashita et al., 1994; Luo and Lodish, 1996; Weis-Garcia and Massagué, 1996; Stockwell and Schreiber, 1998a). Two residues in T $\beta$ R-I, Gly-261 and Gly-322, are required for a functional interaction between T $\beta$ R-I subunits in the ligand-induced receptor complex (Weis-Garcia and Massagué, 1996). Substitution of these amino acids with glutamate and aspartate, respectively, results in a type I receptor that is inactive because it cannot be phosphorylated by T $\beta$ R-II. These activation-defective mutants can be complemented by cotransfection with kinase-inactive T $\beta$ R-I that contains Gly-261 and Gly-322. This implies that the mutations act in *trans*, somehow impeding GS region phosphorylation of the other type I receptor in the tetrameric signaling complex.

The importance of T $\beta$ R-I homooligomerization motivated us to examine the T $\beta$ R-I-FKBP12 crystal lattice for a potentially relevant dimer. One of the dimers generated by noncrystallographic symmetry (NCS) is particularly intriguing (Figure 7). Its interface is fairly extensive,

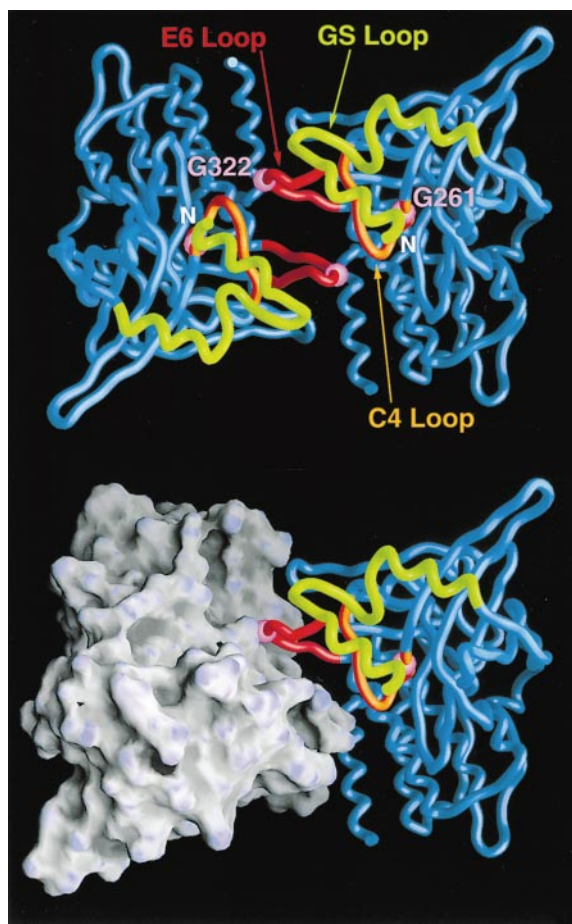


Figure 7. The T $\beta$ R-I NCS Dimer

The dimer is viewed roughly down its two-fold axis. Gly-261 and Gly-322 are shown as magenta spheres. Above, the dimer is shown in ribbon representation, and the N terminus of each protomer is indicated. Below, the molecular surface of the protomer on the left has been included to show the structural complementarity of the dimer interface. FKBP12 is not involved in the formation of this dimer and has been left out of this figure for clarity.

burying a total accessible surface area of  $\sim$ 1860 Å<sup>2</sup>, compared to 1880 Å<sup>2</sup> for the T $\beta$ R-I-FKBP12 interaction. A majority of the dimerization contacts are made by the loop connecting helix  $\alpha$ E and strand  $\beta$ 6 (E6 loop), which bears a characteristic insertion that is, for the most part, conserved among type I receptors (Figure 2). Furthermore, the mutations described above map to the interface of this dimer. Gly-261 is located near the C terminus of the loop connecting  $\alpha$ C and  $\beta$ 4 (C4 loop), while Gly-322 maps to the very tip of the E6 loop. The N termini of both molecules are oriented in the same direction, indicating that this dimer would not be inconsistent with membrane attachment. Gly-261 and Gly-322 are both positioned next to conserved acidic side chains at the dimer interface. Glu-257 from the NCS-related molecule forms a hydrogen bond with the amide nitrogen of Gly-322. Similarly, Gly-261 is positioned next to Asp-281, a residue in the linker connecting  $\beta$ 5 and  $\alpha$ D. It is conceivable that the introduction of negatively charged side chains at these sites could alter the dimer interface as



Table 1. Summary of Crystallographic Analysis

|  |                       | Multiple Isomorphous Replacement         |                             |  |  | FKBP12 Placement                       |                                     |
|--|-----------------------|--|-----------------------------|--|--|--|-------------------------------------|
|  |                       | Native                                   | HgCl <sub>2</sub>           | PCMB   | K <sub>2</sub> PtCl <sub>4</sub>           | Native                                 | SeMet FKBP12                        |
| Resolution (Å)                                   |                       | 30.0–2.8                                 | 30.0–3.6                    | 30.0–3.6   | 30.0–3.5                                   | 30.0–2.6                               | 30.0–2.7                            |
| No. of sites                                     |                       | —  | 12                          | 8  | 4  | —                                      | 12                                  |
| R <sub>sym</sub> (%) <sup>a</sup>                | overall (outer shell) | 7.0 (19.4)                               | 10.2 (23.4)                 | 17.7 (34.8)  | 10.9 (27.6)                                | 8.0 (24.3)                             | 6.6 (18.1)                          |
| Completeness                                     | overall (outer shell) | 97.1 (94.7)                              | 96.9 (96.5)                 | 98.1 (97.1)  | 96.8 (94.4)                                | 98.4 (97.7)                            | 94.8 (85.9)                         |
| I/σ(I)   | overall (outer shell) | 16.7 (4.8)                               | 9.0 (3.2)                   | 6.4 (2.9)  | 8.6 (2.8)                                  | 19.1 (6.0)                             | 16.1 (4.9)                          |
| R <sub>iso</sub> (%) <sup>b</sup>                | —                     | —  | 23.2                        | 18.0   | 21.4                                       | —                                      | 9.8                                 |
| Phasing power <sup>c</sup>                       |                       | —  | 1.7                         | 1.9  | 0.8  | —                                      | —                                   |
| Combined figure of merit (to 3.6 Å) <sup>d</sup> |                       |  |                             |  | 0.42                                       |  |                                     |
| Density Modification                             |                       |  |                             |  |  |  |                                     |
|  |                       | Correlation for Operator #1 <sup>e</sup> | Correlation for Operator #2 | Correlation for Operator #3                              | Final Correlation Coefficient <sup>f</sup> | R Value for NCS Averaging <sup>g</sup> |                                     |
|  |                       | 0.64                                     | 0.23                        | 0.25   | 0.834                                      | 0.240                                  |                                     |
| Refinement                                       |                       |  |                             |  |  |  |                                     |
|  | Resolution Range      | No. of Reflections ( F  > 2σ)            | Total No. of Atoms          | R <sub>working</sub> /R <sub>free</sub> <sup>h</sup> (%) | Rmsd for Bonds (Å)                         | Rmsd for Angles (Deg.)                 | Rmsd for B Values (Å <sup>2</sup> ) |
|  | 30.0–2.6              | 57,740                                   | 13,840                      | 24.9/26.9  | 0.011                                      | 1.66                                   | 1.64                                |

<sup>a</sup> R<sub>sym</sub>% = 100 × Σ|I| - <I>/ΣI, where I is the integrated intensity of a given reflection.

<sup>b</sup> R<sub>iso</sub>% = 100 × Σ|F<sub>PH</sub> - F<sub>P</sub>|/ΣF<sub>P</sub>, where F<sub>PH</sub> and F<sub>P</sub> are the derivative and native structure factor amplitudes, respectively.

<sup>c</sup> Phasing power = Σ|F<sub>PH</sub>|/Σ|F<sub>PH</sub>(obs) - |F<sub>PH</sub>(calc)||, where F<sub>PH</sub> is the calculated heavy atom structure factor amplitude.

<sup>d</sup> Figure of merit = <|ΣP(α)e<sup>iα</sup>/Σ|P(α)|>, where α is the phase and P(α) is the phase probability distribution.

<sup>e</sup> Correlation coefficient for an NCS operator = {Σ(p<sub>a</sub> - <p>)(p<sub>b</sub> - <p>)} / {Σ(p<sub>a</sub> - <p>)<sup>2</sup> Σ(p<sub>b</sub> - <p>)<sup>2</sup>}<sup>1/2</sup>, where p<sub>a</sub> and p<sub>b</sub> represent electron density related by the NCS operator in question.

<sup>f</sup> Correlation coefficient = {Σ(F(obs) - <F(obs)>)(F(calc) - <F(calc)>)} / {Σ(F(obs) - <F(obs)>)<sup>2</sup> Σ(F(calc) - <F(calc)>)<sup>2</sup>}<sup>1/2</sup>, where F(calc) represents the structure factor amplitudes obtained from back-transformation of NCS averaged maps.

<sup>g</sup> R value = Σ|F(obs) - F(calc)|/ΣF(obs), where F(calc) is defined as in<sup>f</sup>.

<sup>h</sup> R value = Σ|F(obs) - F(calc)|/ΣF(obs), where F(calc) represents the structure factor amplitudes obtained from back-transformation of the model. The free R value was calculated using 10% of the data.

it is seen in the structure. This could, in turn, affect GS loop phosphorylation by TβR-II.

## Conclusions

The utilization of tyrosine kinases as receptors for polypeptide ligands is a specialization that is unique to intercellular communication in metazoans (Hanks and Hunter, 1995). It is notable that TGFβ family receptors, which also transduce signals delivered by polypeptide ligands, function as serine/threonine-specific rather than tyrosine-specific kinases. The classification of protein kinases on the basis of primary sequences had revealed a connection between the catalytic domains of receptors of the TGFβ family and those of the tyrosine kinases (Hanks and Hunter, 1995). The structure described here now makes clear that the location in TβR-I of the catalytic segment and, by implication, the bound nucleotide, resembles that seen in tyrosine kinases rather than serine/threonine kinases. This result appears to be a consequence of dispersed changes in amino acid sequence rather than localized alterations of sequence motifs. The idea that functional similarities can exist in the absence of subtype-specific residues has been established by the analyses of various dual specificity kinases (Lindberg et al., 1992). The TβR-I-FKBP12 structure illustrates how this phenomenon can be manifested in three dimensions. The active site configuration of TβR-I appears to be consistent with binding both tyrosine as well as the smaller serine and threonine side

chains, as suggested by previous biochemical analyses for the related type II receptor (Lawler et al., 1997).

Members of the type I family of TGFβ receptors are also distinguished from receptor tyrosine kinases by virtue of a unique regulatory mechanism, which involves phosphorylation by the type II receptors of a short N-terminal segment (the GS region). Receptor tyrosine kinases are activated by phosphorylation within the centrally located activation segment of the kinase domain, which blocks or distorts the active site when unphosphorylated (Hubbard et al., 1994; Mohammadi et al., 1996; Hubbard, 1997). In contrast, the regulatory GS region of TβR-I is located distal to the active site. Nevertheless, the GS region is seen to be coupled structurally to the activation segment by helix αC in the N lobe. The manipulation of the αC helix and the activation segment by regulatory inputs is a common theme in protein kinase regulation (Jeffrey et al., 1995; Johnson et al., 1996; Sicheri et al., 1997; Xu et al., 1997), and in TβR-I the displacement of αC by the unphosphorylated GS region is correlated with an inhibitory conformation of the activation segment. The structure of TβR-I demonstrates that one key role for phosphorylation is to block the adoption of an inactivating configuration by the GS region. The structure does, however, leave unanswered the question of how the phosphorylated GS region participates in the action of the assembled heteromeric receptor complex, which remains a challenge for future structural analyses.

## Experimental Procedures

### Protein Expression and Purification

The cytoplasmic domain of human T $\beta$ R-I (residues 162–503, hereafter called T $\beta$ R-I) was produced in SF9 cells using a baculoviral expression system (Bac-to-Bac, GIBCO). Cells were lysed by sonication in 50 mM Tris (pH 8.5), 50 mM NaCl, 10 mM MgCl<sub>2</sub>, 8% glycerol, 2 mM DTT, 1 mM phenyl-methyl sulphonyl fluoride. The soluble fraction of the lysate was applied to a Q sepharose column attached in tandem with a  $\gamma$ -phosphate conjugated ATP column. Q sepharose does not bind T $\beta$ R-I under these conditions and functioned as a subtractive step in the purification. After loading, the ATP column was eluted with a gradient of salt and EDTA. Fractions containing T $\beta$ R-I were pooled; the protein was concentrated by ultrafiltration and then applied to a HiLoad Superdex 75 column (Pharmacia). Purified T $\beta$ R-I can be concentrated to 80 mg/ml.

Full-length human FKBP12 was overexpressed in *E. coli* and purified using, in turn, Q sepharose, phenyl sepharose, and gel filtration chromatography. Selenomethionine FKBP12 was prepared in a similar fashion, and full SeMet incorporation was confirmed by electrospray mass spectrometry. T $\beta$ R-I–FKBP12 complex was generated by adding an excess of FKBP12 to T $\beta$ R-I and applying the resultant mixture to a sizing column equilibrated in 20 mM Tris (pH 7.5), 150 mM NaCl, 2 mM DTT. The two proteins coelute from a Superdex 75 HR 10/30 column (Pharmacia) as a stoichiometric complex.

### Crystallization and Data Collection

Crystallization trials using T $\beta$ R-I alone yielded plate-like crystals that were difficult to handle and diffracted X-rays weakly. Subsequent proteolysis experiments showed that FKBP12 afforded T $\beta$ R-I an appreciable amount of proteolytic protection, indicating that the T $\beta$ R-I–FKBP12 complex would likely be a better crystallization target. Crystals of the T $\beta$ R-I–FKBP12 complex were obtained at 20°C using a reservoir solution of 100 mM Tris (pH 8.3–8.6), 1.40–1.53 M (NH<sub>4</sub>)<sub>2</sub>SO<sub>4</sub>. T $\beta$ R-I–FKBP12 complex was diluted to 20 mg/ml in a buffer containing 10 mM MgCl<sub>2</sub> and 2 mM AMP-PNP. (Although not apparently incorporated into the crystals, the nucleotide slightly improves crystal morphology.) Equal volumes of protein and reservoir solution were combined with a half volume of 0.5 M NaI in the crystallization drop. The presence of NaI was absolutely essential for the growth of diffraction quality crystals. Crystals tended to grow in large clusters, from which small single chunks (0.05–0.15 mm on each edge) could be removed by surgery. The crystals were stabilized in 100 mM Tris (pH 8.5), 1.7 M (NH<sub>4</sub>)<sub>2</sub>SO<sub>4</sub>, 100 mM NaI, and either stream frozen or propane frozen after a short incubation in the same solution plus 25% ethylene glycol.

X-ray data used to solve the structure were collected using frozen crystals at a laboratory copper K $\alpha$  source (Rigaku RU 200) and at the X25 beamline at the National Synchrotron Light Source (NSLS). Data were processed using DENZO and SCALEPACK (Otwinowski and Minor, 1997). T $\beta$ R-I–FKBP12 crystallizes in the triclinic space group P1 ( $a = 75.6 \text{ \AA}$ ,  $b = 81.1 \text{ \AA}$ ,  $c = 90.5 \text{ \AA}$ ,  $\alpha = 86.2^\circ$ ,  $\beta = 81.9^\circ$ ,  $\gamma = 63.9^\circ$ ) with four 1:1 complexes in the asymmetric unit and a solvent content of 52%. The crystals are pseudomonoclinic, and data were initially processed in the space group C2. This resulted in a large number of rejected reflections, unstable SCALEPACK postrefinement, and unacceptably poor statistics at high resolution. Examination of Bijvoet pairs, given C2 symmetry, revealed implausible differences in intensity, demonstrating that the crystals were triclinic.

### Structure Determination and Refinement

The structure was solved using multiple isomorphous replacement (MIR) with placement of FKBP12 by selenium difference Fourier (see Table 1). A self-rotation function of the native data revealed three perpendicular noncrystallographic symmetry (NCS) two-fold axes. A derivative was obtained using HgCl<sub>2</sub>, and the difference Patterson solution gave six pairs of sites, each related by the most prominent two-fold. This established the first NCS operator. The program FIND\_NCS (Lu, 1999) was used to locate the other two operators. A data set for crystals of SeMet FKBP12–T $\beta$ R-I was collected, and a difference map was calculated using phases from the HgCl<sub>2</sub> derivative. Knowledge of the NCS symmetry within the unit cell allowed

the unambiguous assignment of the FKBP12 methionine positions. Two additional derivatives, K<sub>2</sub>PtCl<sub>6</sub> and PCMB, were obtained and, with the HgCl<sub>2</sub> phases included, gave a combined initial figure of merit of 0.42.

Phases from the mercury and platinum derivatives were calculated to 3.6 Å using MLPHARE (CCP4, 1994) and SHARP (La Fortelle and Bricogne, 1997). The initial experimental map was uninterpretable, but rough protomer–solvent boundaries could be distinguished. A protomer mask was generated in MAMA (Kleywegt and Jones, 1993), and the density was four-fold averaged using RAVE (Kleywegt and Read, 1998). The resultant map confirmed the initial FKBP12 placement and allowed initiation of an iterative procedure of model building, constrained refinement in CNS (Brünger et al., 1998), phase combination, mask improvement, and four-fold averaging with phase extension to 3.0 Å.

Refinement with tight NCS restraints was carried out using data to 2.6 Å (X25, NSLS). Three rigid bodies (FKBP12, kinase N lobe, and kinase C lobe) were used to define the NCS restraints. The current model contains residues 1–107 of FKBP12 and 175–500 of T $\beta$ R-I, a total of 13,840 nonhydrogen atoms, including 88 water molecules and four sulfate ions. The average temperature factors for all atoms of T $\beta$ R-I and FKBP12 are 35 Å<sup>2</sup> and 42 Å<sup>2</sup>, respectively. Three small portions of the kinase—the phosphate-binding loop, the L45 loop, and the very C terminus—display high temperature factors (~80 Å<sup>2</sup>). The electron density, though, is quite good in all of these regions with the exception of two residues at the very tip of the L45 loop, G271 and T272, which exhibit the highest B factors in the entire protein complex. The occupancies of some surface side chain atoms (D269, Q324, K343, H371, and K391 from T $\beta$ R-I; Q3 and K52 from FKBP12) have been set to 0 on account of poor density. The model has been refined to a working R value of 24.9% and a free R value of 26.9%. The R value is relatively high and reflects the fact that very tight NCS restraints were imposed for the entire refinement (rms deviations of ~0.003 Å between C $\alpha$  positions for NCS-related rigid bodies in the final structures). 88.6% of protein residues are in the most favored regions of the Ramachandran plot, with none in the disallowed regions.

### Acknowledgments

We thank C. Harrison for initial work on T $\beta$ R-I expression, H. Viguet for technical assistance, T. Muir for use of the electrospray mass spectrometer, and A. Hemmati-Brivanlou for the Ire1p observation. L. Berman, B. Sweet, and the staff of the National Synchrotron Light Source are gratefully acknowledged for assistance with synchrotron data collection. Additional thanks go to D. Jeruzalmi, S. Soisson, J. Bonanno, E. Conti, T. Schindler, X. Chen, A. Boriack-Sjodin, H. Yamaguchi, Y. Zhao, F. Sicheri, S. K. Burley, S. Nair, J. Marcotrigiano, and J. Gulbis for help and advice. M. H. is a National Science Foundation predoctoral fellow. Additional support was supplied by National Institutes of Health grants to J. M. (CA34610) and to the Memorial Sloan Kettering Cancer Center.

Received November 16, 1998; revised December 24, 1998.

### References

- Armstrong, R.N., Kondo, H., Granot, J., Kaiser, E.T., and Mildvan, A.S. (1979). Magnetic resonance and kinetic studies of the manganese II ion and substrate complexes of the catalytic subunit of adenosine 3',5'-monophosphate dependent protein kinase from bovine heart. *Biochemistry* 18, 1230–1238.
- Brünger, A.T. (1992). The free R value: a novel statistical quantity for assessing the accuracy of crystal structures. *Nature* 355, 472–474.
- Brünger, A.T., Adams, P.D., Clore, G.M., Gros, P., Grosse-Kuntze, R.W., Jiang, J.-S., Kuszewski, J., Nilges, M., Pannu, N.S., Read, R.J., et al. (1998). Crystallographic and NMR system: a new software system for macromolecular structure determination. *Acta Crystallogr. D54*, 905–921.
- Carson, M. (1991). Ribbons 2.0. *J. Appl. Crystallogr.* 24, 958–961.
- CCP4 (1994). The CCP4 suite: programs for protein crystallography. *Acta Crystallogr. D50*, 760–763.

- Charng, M.-J., Kinnunen, P., Hawker, J., Brand, T., and Schneider, M.D. (1996). FKBP-12 recognition is dispensable for signal generation by type I transforming growth factor- $\beta$  receptors. *J. Biol. Chem.* **271**, 22941–22944.
- Chen, R.-H., and Derynck, R. (1994). Homomeric interactions between type II transforming growth factor- $\beta$  receptors. *J. Biol. Chem.* **269**, 22868–22874.
- Chen, F., and Weinberg, R.A. (1995). Biochemical evidence for the autophosphorylation and transphosphorylation of transforming growth factor beta receptor kinases. *Proc. Natl. Acad. Sci. USA* **92**, 1565–1569.
- Chen, Y.-G., Liu, F., and Massagué, J. (1997). Mechanism of TGF- $\beta$  receptor inhibition by FKBP12. *EMBO J.* **16**, 3866–3876.
- Chen, Y.-G., Hata, A., Lo, R.S., Wotton, D., Shi, Y., Pavletich, N., and Massagué, J. (1998). Determinants of specificity in TGF- $\beta$  signal transduction. *Genes Dev.* **12**, 2144–2152.
- Feng, X.-H., and Derynck, R. (1997). A kinase subdomain of transforming growth factor- $\beta$  (TGF- $\beta$ ) type I receptor determines the TGF- $\beta$  intracellular signaling specificity. *EMBO J.* **16**, 3912–3923.
- Feng, X.-H., Filvaroff, E.H., and Derynck, R. (1995). Transforming growth factor- $\beta$  (TGF- $\beta$ )-induced down-regulation of cyclin A expression requires a functional TGF- $\beta$  receptor complex. *J. Biol. Chem.* **270**, 24237–24245.
- Goldberg, J., Nairn, A.C., and Kuriyan, J. (1996). Structural basis for the autoinhibition of calcium/calmodulin-dependent protein kinase I. *Cell* **84**, 875–887.
- Griffith, J.P., Kim, J.L., Kim, E.E., Sintchak, M.D., Thomson, J.A., Fitzgibbon, M.J., Fleming, M.A., Caron, P.R., Hsiao, K., and Navia, M.A. (1995). X-ray structure of calcineurin inhibited by the immunophilin-immunosuppressant FKBP12-FK506 complex. *Cell* **82**, 507–522.
- Hanks, S.K., and Hunter, T. (1995). The eukaryotic protein kinase superfamily: kinase (catalytic) domain structure and classification. *FASEB J.* **9**, 576–596.
- Harrison, R.K., and Stein, R.L. (1990). Substrate specificities of the peptidyl prolyl cis-trans isomerase activities of cyclophilin and FK-506 binding protein: evidence for the existence of a family of distinct enzymes. *Biochemistry* **29**, 3813–3816.
- Heldin, C.H., Miyazono, K., and ten Dijke, P. (1997). TGF- $\beta$  signaling from cell membrane to nucleus through SMAD proteins. *Nature* **390**, 465–471.
- Henis, Y.I., Moustakas, A., Lin, H.Y., and Lodish, H.F. (1994). The type II and III transforming growth factor- $\beta$  receptors form homooligomers. *J. Cell. Biol.* **126**, 139–154.
- Hu, S.-H., Parker, M.W., Lei, J.Y., Wilce, M.C.J., Benian, G.M., and Kemp, B.E. (1994). Insights into autoregulation from the crystal structure of twitchin kinase. *Nature* **369**, 581–584.
- Hubbard, S.R. (1997). Crystal structure of the activated insulin receptor tyrosine kinase in complex with peptide substrate and ATP analog. *EMBO J.* **16**, 5572–5581.
- Hubbard, S.R., Wei, L., Ellis, L., and Hendrickson, W.A. (1994). Crystal structure of the tyrosine kinase domain of the human insulin receptor. *Nature* **372**, 746–754.
- Jeffrey, P.D., Russo, A.A., Polyak, K., Gibbs, E., Hurwitz, J., Massagué, J., and Pavletich, N.P. (1995). Mechanism of CDK activation revealed by the structure of a cyclinA-CDK2 complex. *Nature* **376**, 313–320.
- Johnson, L.N., Noble, M.E.M., and Owen, D.J. (1996). Active and inactive protein kinases: structural basis for regulation. *Cell* **85**, 149–158.
- Kleywegt, G.J., and Jones, T.A. (1993). Masks made easy. *ESF/CCP4 Newsletter*, 56–59.
- Kleywegt, G.J., and Read, R.J. (1998). Not your average density. *Structure* **5**, 1557–1569.
- Knighton, D.R., Zheng, J., Ten Eyck, L.F., Ashford, V.A., Xuong, N.-H., Taylor, S.S., and Sowadski, J.M. (1991). Crystal structure of the catalytic subunit of cyclic adenosine monophosphate-dependent protein kinase. *Science* **253**, 407–414.
- Kretschmar, M., Liu, F., Hata, A., Doody, J., and Massagué, J. (1997). The BMP mediator Smad1 is phosphorylated directly and activated functionally by the BMP receptor kinase. *Genes Dev.* **11**, 984–995.
- La Fortelle, E.D., and Bricogne, G. (1997). Maximum-likelihood heavy-atom parameter refinement in the MIR and MAD methods. *Methods Enzymol.* **276**, 472–494.
- Lawler, S., Feng, X.-H., Chen, R.-H., Maruoka, E.M., Turck, C.W., Griswold-Prenner, I., and Derynck, R. (1997). The type II transforming growth factor- $\beta$  receptor autophosphorylates not only on serine and threonine but also on tyrosine residues. *J. Biol. Chem.* **272**, 14850–14859.
- Lindberg, R.A., Quinn, A.M., and Hunter, T. (1992). Dual-specificity kinases: will any hydroxyl do? *Trends Biochem. Sci.* **17**, 114–119.
- Livingston, C.D., and Barton, G.J. (1996). Identification of functional residues and secondary structure from protein multiple sequence alignment. *Methods Enzymol.* **266**, 497–512.
- Lu, G. (1999). FIND\_NCS: a program which automatically finds out the NCS operation from heavy atom sites, in press.
- Luo, K., and Lodish, H.F. (1996). Signaling by chimeric erythropoietin-TGF- $\beta$  receptors: homodimerization of the cytoplasmic domain of the type I TGF- $\beta$  receptor and heterodimerization with the type II receptor are both required for intracellular signal transduction. *EMBO J.* **15**, 4485–4496.
- Massagué, J. (1990). The transforming growth factor- $\beta$  family. *Annu. Rev. Cell Biol.* **6**, 597–641.
- Massagué, J. (1998). TGF- $\beta$  signal transduction. *Annu. Rev. Biochem.* **67**, 753–791.
- Mohammadi, M., Schlessinger, J., and Hubbard, S.R. (1996). Structure of the FGF receptor tyrosine kinase domain reveals a novel autoinhibitory mechanism. *Cell* **86**, 577–587.
- Nicholls, A., Sharp, K.A., and Honig, B. (1991). Protein folding and association: insights from the interfacial and thermodynamic properties of hydrocarbons. *Proteins: Struct. Funct. Genet.* **11**, 281–296.
- Okadome, T., Oeda, E., Saitoh, M., Ichijo, H., Moses, H.L., Miyazono, K., and Kawabata, M. (1996). Characterization of the interaction of FKBP12 with the transforming growth factor- $\beta$  type I receptor in vivo. *J. Biol. Chem.* **271**, 21687–21690.
- Otwinowski, Z., and Minor, W. (1997). Processing of X-ray diffraction data collected in oscillation mode. *Methods Enzymol.* **276**, 307–326.
- Owen, D.J., Noble, M.E.M., Garman, E.F., Papageorgiou, A.C., and Johnson, L.N. (1995). Two structures of the catalytic domain of phosphorylase kinase: an active protein kinase complexed with substrate analogue and product. *Structure* **3**, 467–482.
- Roberts, A.B., and Sporn, M.B. (1990). The transforming growth factor-betas. In *Peptide Growth Factors and Their Receptors*, M.B. Sporn and A.B. Roberts, eds. (Heidelberg: Springer-Verlag), pp. 419–472.
- Russo, A.A., Jeffrey, P.D., Patten, A.K., Massagué, J., and Pavletich, N.P. (1996). Crystal structure of the p27Kip1 cyclin-dependent-kinase inhibitor bound to the cyclin A-Cdk2 complex. *Nature* **382**, 325–331.
- Schreiber, S.L. (1991). Chemistry and biology of the immunophilins and their immunosuppressive ligands. *Science* **251**, 283–287.
- Shamu, C.E., and Walter, P. (1996). Oligomerization and phosphorylation of the Ire1p kinase during intracellular signaling from the endoplasmic reticulum to the nucleus. *EMBO J.* **15**, 3028–3039.
- Shou, W., Aghdasi, B., Armstrong, D.L., Guo, Q., Bao, S., Charng, M.-J., Mathews, L.M., Schneider, M.D., Hamilton, S.L., and Matzuk, M.M. (1998). Cardiac defects and altered ryanodine receptor function in mice lacking FKBP12. *Nature* **391**, 489–492.
- Sicheri, F., Moarefi, I., and Kuriyan, J. (1997). Crystal structure of the Src family tyrosine kinase Hck. *Nature* **385**, 602–609.
- Souchelnytskyi, S., ten Dijke, P., Miyazono, K., and Heldin, C.-H. (1996). Phosphorylation of Ser165 in TGF- $\beta$  type I receptor modulates TGF- $\beta$ 1-induced cellular responses. *EMBO J.* **15**, 6231–6240.
- Stockwell, B.R., and Schreiber, S.L. (1998a). Probing the role of homomeric and heteromeric receptor interactions in TGF- $\beta$  signaling using small molecule dimerizers. *Curr. Biol.* **8**, 761–770.
- Stockwell, B.R., and Schreiber, S.L. (1998b). TGF- $\beta$ -signaling with



small molecule FKBP12 antagonists that bind myristoylated FKBP12-TGF- $\beta$ -type I receptor fusion proteins. *Chem. Biol.* **5**, 385–395.

Van Duyne, G.D., Standaert, R.F., Karplus, P.A., Schreiber, S.L., and Clardy, J. (1991). Atomic structure of FKBP-FK506, an immunophilin-immunosuppressant complex. *Science* **252**, 839–842.

Wang, T., Donahoe, P.K., and Zervos, A.S. (1994). Specific interaction of type I receptors of the TGF- $\beta$  family with the immunophilin FKBP12. *Science* **265**, 674–676.

Wang, T., Li, B.-Y., Danielson, P.D., Shah, P.C., Rockwell, S., Lechleider, R.J., Martin, J., Manganaro, T., and Donahoe, P.K. (1996). The immunophilin FKBP12 functions as a common inhibitor of the TGF $\beta$  family type I receptors. *Cell* **86**, 435–444.

Wang, Z., Harkins, P.C., Ulevitch, R.J., Han, J., Cobb, M.H., and Goldsmith, E.J. (1997). The structure of mitogen-activated protein kinase p38 at 2.1 Å resolution. *Proc. Natl. Acad. Sci. USA* **94**, 2327–2332.

Weis-Garcia, F., and Massagué, J. (1996). Complementation between kinase-defective and activation-defective TGF- $\beta$  receptors reveals a novel form of receptor cooperativity essential for signaling. *EMBO J.* **15**, 276–289.

Wieser, R., Wrana, J.L., and Massagué, J. (1995). GS domain mutations that constitutively activate T $\beta$ R-I, the downstream signaling component in the TGF- $\beta$  receptor complex. *EMBO J.* **14**, 2199–2208.

Willis, S.A., Zimmerman, C.M., Li, L., and Mathews, L.S. (1996). Formation and activation by phosphorylation of activin receptor complexes. *Mol. Endocrinol.* **10**, 367–379.

Wilson, K.P., Yamashita, M.M., Sintchak, M.D., Rotstein, S.H., Murcko, M.A., Boger, J., Thomson, J.A., Fitzgibbon, M.J., Black, J.R., and Navia, M.A. (1995). Comparative X-ray structures of the major binding protein for the immunosuppressant FK506 (tacrolimus) in unligated form and in complex with FK506 and rapamycin. *Acta Crystallogr. D* **51**, 511–521.

Wrana, J.L., Attisano, L., Wieser, R., Ventura, F., and Massagué, J. (1994). Mechanism of activation of the TGF- $\beta$  receptor. *Nature* **370**, 341–347.

Xu, W., Harrison, S.C., and Eck, M.J. (1997). Three-dimensional structure of the tyrosine kinase c-Src. *Nature* **385**, 595–602.

Yamashita, H., ten Dijke, P., Franzen, P., Miyazano, K., and Heldin, C.-H. (1994). Formation of hetero-oligomeric complexes of type I and type II receptors for transforming growth factor- $\beta$ . *J. Biol. Chem.* **269**, 20172–20178.

Zheng, J., Knighton, D.R., Ten Eyck, L.F., Karlsson, R., Xuong, N.-H., Taylor, S.S., and Sowadski, J.M. (1993). Crystal structure of the catalytic subunit of c-AMP-dependent protein kinase complexed with Mg/ATP and peptide inhibitor. *Biochemistry* **32**, 2154–2161.

#### Brookhaven Protein Data Bank ID Code

The coordinates for the structure described in this paper have been deposited with the ID code 1b6c. The coordinates may also be obtained at the website (<http://www.rockefeller.edu/kuriyan>).